Track Nanomembranes and Secondary Structures on Their Base as Nanomaterials

Mchedlishvili, B.V.; Asadchikov, V.E.; Vilensky, A.I.; Vasil'ev, A.B.; Zagorski, D.L.; Nechaev, A.N.; Oleinikov, V.A.; Sergeev, A.V.; Popok, Vladimir; Samotolin, N.D.; Melnik, N.N.

Published in:
Crystallography Reports

Publication date:
2003

Document Version
Publisher's PDF, also known as Version of record

Crystallography Reports, Vol. 48, Suppl. 1, 2003, pp. S140–S148. Translated from Kristallografiya, Vol. 48, No. 6 (Suppl.), 2003, pp. S153–S161.

NANOMATERIALS

Dedicated to the 60th Anniversary of the Shubnikov Institute of Crystallography, Russian Academy of Sciences

Track Nanomembranes and Secondary Structures on Their Base as Nanomaterials

B. V. Mchedlishvili*, V. E. Asadchikov*, A. I. Vilenskiĭ*, A. B. Vasil'ev*, D. L. Zagorskiĭ*, A. N. Nechaev*, V. A. Oleĭnikov, A. V. Sergeev*, V. N. Popok***, N. D. Samotolin****, and N. N. Mel'nik*******

* *Shubnikov Institute of Crystallography, Russian Academy of Sciences, Leninskiĭ pr. 59, Moscow, 119333 Russia*

e-mail: track@imb.ac.ru

** *Shemyakin–Ovchinnikov Institute of Bioorganic Chemistry, Russian Academy of Sciences, ul. Miklukho-Maklaya 16/10, Moscow, 117871 Russia*

*** *Belarussian State University, pr. F. Skoriny 4, Minsk, 220050 Belarus*

**** *Institute of Geology of Ore Deposits, Petrography, Mineralogy, and Geochemistry (IGEM), Russian Academy of Sciences, Staromonetnyĭ per. 35, Moscow, 109017 Russia*

***** *Lebedev Physical Institute, Russian Academy of Sciences, Leninskiĭ pr. 53, Moscow, 119924 Russia*

Received June 5, 2003

Abstract—This paper gives a brief history of the development of track nanomembranes in 1983–2003, followed by an analysis of the results of investigations into the transformation of the crystal structure of thin polymer films (initial materials used in the preparation of track membranes) under both irradiation with high-energy particles (ions, fission fragments) at energies ranging from 1 to 3 MeV/amu and synchrotron radiation. The currently available data on the modification of the properties of thin crystal layers of inorganic materials upon their interaction with high-energy, multiply charged, heavy ions at particle energies from 300 to 700 MeV are considered. It is demonstrated that track nanomembranes can be used in cleaning of crystallization solutions (for the growth of organic and inorganic crystals), biotechnology, medicine, and nanotechnology. © *2003 MAIK "Nauka/Interperiodica".*

INTRODUCTION

As a rule, nanomaterials are considered structures or materials exhibiting qualitatively new properties due to a decrease in the size (in one or several dimensions) of the objects to a nanometer scale. According to the modern classification, nanomaterials are objects with characteristic sizes of 100 nm or less [1].

In the early 1960s, Price and Walker [2] published the first data on the preparation of track membranes. Thin polymer films were irradiated with fission fragments, and, then (as is customary when producing solid-state detectors of this type), the tracks thus prepared were etched until surface or through pores were formed. The research works performed under the supervision of G.N. Flerov in 1973–1983 demonstrated the prospects of using nonradioactive high-energy heavy ions instead of radioactive fission fragments [3]. These ions were accelerated to energies of 1–2 MeV/amu on cyclic, linear, or electrostatic charge-exchange accelerators. It was necessary to investigate the particular stages of preparing track membranes in greater detail and to reduce them to practice. For this purpose, in 1983, the Laboratory of Nuclear Filters (the old name of track membranes)—now, the Department of Membrane Technologies—was organized at the Shubnikov Institute of Crystallography of the USSR Academy of Sciences.

In 1993–1994, Ch.R. Martin and researchers of the Shubnikov Institute of Crystallography of the Russian Academy of Sciences (see [4, 5]) described track membranes as nanomaterials for the first time. In actual fact, track membranes are typical nanomaterials: the sizes of membrane pores range from several nanometers (a hollow track channel) to tens or several hundreds of nanometers (track nanomembranes). In particular, it was demonstrated that secondary nanostructures (systems of tips, cylinders, nanotubes, nanowires) can be prepared by the replica (template) method using a system of calibrated pores of track membranes [4–6].

1063-7745/03/48S1-S0140$24.00 © 2003 MAIK "Nauka/Interperiodica"

The results of the investigations carried out in recent years have shown that it is necessary not only to analyze the changes observed in the properties of polymers and crystals at the stage of transforming a system of tracks into a system of pores but also to obtain detailed and reliable information on structural transformations of these materials directly in regions of latent tracks. It is these data that will make it possible to predict and improve the structure and properties of both track membranes and secondary nanostructures.

STRUCTURAL TRANSFORMATIONS IN POLYMERS UNDER IRRADIATION WITH HIGH-ENERGY PARTICLES

A large number of works have been concerned with the interaction of high-energy ions with polymers used in the preparation of track membranes [7, 8]. However, a number of problems associated with the structural transformations occurring in polymers after their irradiation with accelerated heavy ions remain to be solved. In this section, we will discuss the results of investigations into the structural transformations observed in poly(ethylene terephthalate), polycarbonate, and polyimide under irradiation with accelerated, multiply charged, heavy ions. Moreover, we present the results of our comparative studies of latent tracks in polymers and crystals.

For the most part, irradiated crystals, polymers, and secondary structures have been investigated by infrared (IR), ultraviolet (UV), electron paramagnetic resonance (EPR), and surface-enhanced Raman spectroscopy and atomic force microscopy (AFM). Distler *et al.* [9] studied the surface of mica and its cleavages by the gold decoration technique. Furthermore, the surfaces of fused silica and leucosapphire samples were examined using X-ray scattering [10].

It is known that, under irradiation with heavy ions, the crystal structure of poly(ethylene terephthalate) undergoes transformations. The degree and character of these transformations were evaluated from the ratios of the optical densities D of the polymer ($D_1 = D_{1473}/D_{1455}$, $D_2 = D_{1343}/D_{1370}$), which were measured at characteristic frequencies in the IR spectra of the *trans* (1473, 1343 cm^{-1}) and *gauche* (1455, 1370 cm^{-1}) conformations of CH_2 groups (Fig. 1). The drastic decrease in these ratios with an increase in the ion fluence above 10^9 cm^{-2} is associated with the increase in the fraction of *gauche* conformations after irradiation of the polymer and, hence, with its amorphization.

Heat treatment of polymers can also result in a transformation of their crystal structure. For poly(ethylene terephthalate), the degree of crystallinity was estimated from the ratio $D_3 = D_{988}/D_{873}$. A decrease in the optical-density ratio with an increase in the temperature indicates that poly(ethylene terephthalate) undergoes crystallization. It is established that the polymers subjected to irradiation begin to crystallize at lower temperatures and the crystallization proceeds at higher rates as compared to unirradiated polymers (Fig. 2). A similar dependence is observed for the poly(ethylene terephthalate) samples irradiated with fission fragments of uranium nuclei.

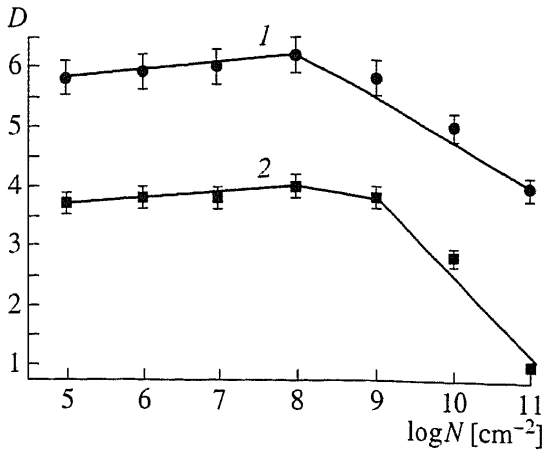

Fig. 1. Dependences of the ratios (*1*) D_1 and (2) D_2 on the xenon ion fluence for poly(ethylene terephthalate) (ion energy, 1 MeV/amu).

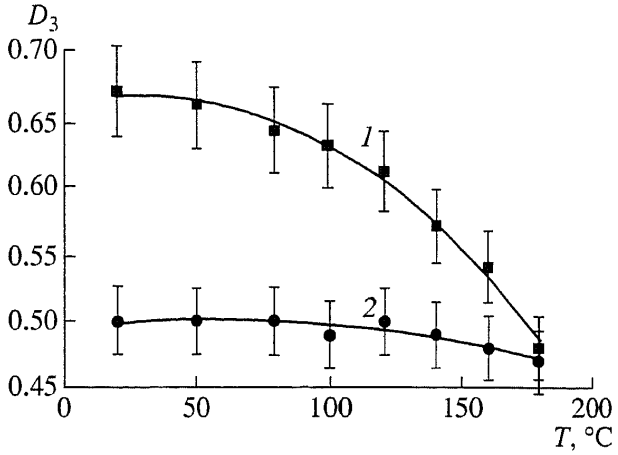

Fig. 2. Temperature dependences of the ratio D_3 for (*1*) the poly(ethylene terephthalate) sample irradiated with xenon ions at a fluence of 10^{11} cm^{-2} (annealing time, 3 h) and (2) unirradiated sample.

Most likely, this effect of annealing can be caused by the fact that irradiation of the polymer results in the destruction of macromolecules, which is accompanied by the removal of part of the low-molecular gaseous products and the formation of regions with a lower density of the material around the tracks of ions. In the track regions, the macromolecules transform into a nonequilibrium (amorphous) state. Heat treatment at temperatures above the glass transition point of the polymer provides conditions for a more regular packing of the polymer macromolecules in track regions with a lower density.

The luminescence background revealed in the Raman spectra of irradiated poly(ethylene terephthalate) films indicates that tracks contain graphite in the form of nanoparticles [11]. The EPR spectra of

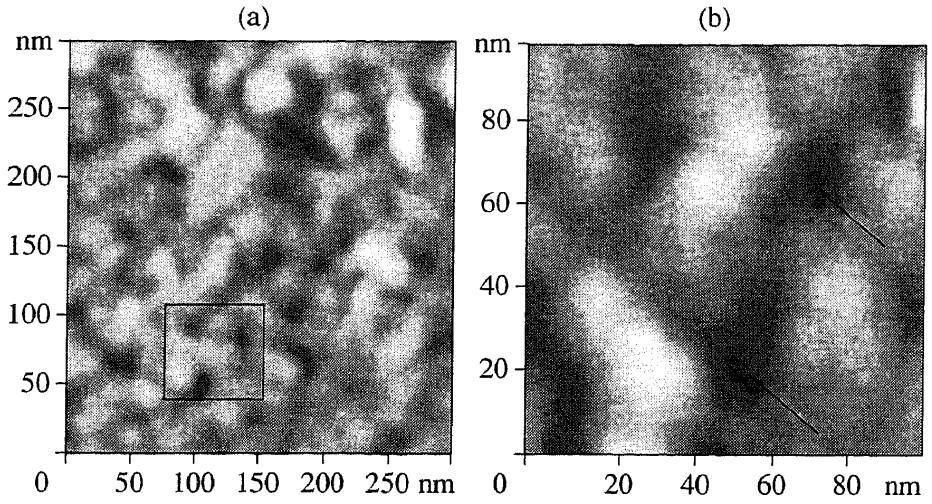

Fig. 3. (a) AFM image of the surface of the poly(ethylene terephthalate) sample irradiated with xenon ions (scanned area, 250 × 250 nm). (b) AFM image of the surface region. Arrows indicate entrance holes for high-energy heavy ions on the polymer surface.

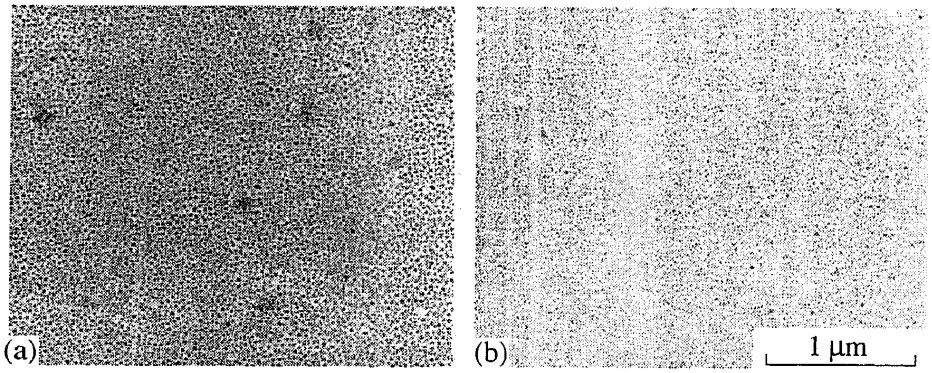

Fig. 4. Topography of the surface of the mica (muscovite) sample decorated with gold through vacuum evaporation: (a) mica irradiated with xenon ions at a fluence of 10^9 cm^{-2} and (b) unirradiated mica (reference sample).

poly(ethylene terephthalate) samples irradiated with xenon ions exhibit a signal with $g = 2.0036 \pm 0.0005$ and a linewidth of approximately 10 G. This signal is due to the radiation-induced breaking of bonds in irradiated graphite with a defect surface [12]. After etching of latent tracks to a diameter of 50 nm, the above EPR signal becomes weaker and broader but does not disappear. This means that the size of modified track regions in the polymer is greater than 50 nm. Similar regularities are also revealed in polycarbonate irradiated with krypton ions.

A different situation is observed for polyimide irradiated with accelerated ions. We found that the intensity of the amorphous-sensitive band at 726 cm^{-1} decreases with an increase in the ion fluence. This suggests that irradiation of the polyimide encourages crystallization of the polymer.

The formation of ordered structures in polymers subjected to irradiation with heavy ions was examined by measuring the intensity ratios of dichroic absorption bands. For a polyimide film, these bands were observed at frequencies of 726, 1380, 1512, and 1776 cm^{-1} in the case when the angles between the film plane and the incident beam were equal to 90° and 45°. These studies revealed a general tendency: the intensity ratios of dichroic bands are virtually independent of the ion fluence at a normal orientation of the film with respect to the incident beam of IR radiation but increase with increasing ion fluence when samples are oriented at an angle of 45° with respect to the ion beam. This implies that the orientation of ordered structures formed as a result of ion irradiation is unrelated to the drawing of the film in the course of the preparation but is determined solely by the direction of ion migration through the polymer. An increase in the intensity ratios of the dichroic bands with an increase in the surface irradiation density indicates that ions passing through the polymer orient the macromolecules along the track axes.

Similar changes are also observed in the polymers studied upon exposure to synchrotron radiation.

Irradiation with high-energy heavy ions brings about changes in the topography of solid surfaces and is attended by the formation of radiation-induced defects, namely, tracks. The images of the entrance holes produced by xenon ions on the surface of the poly(ethylene terephthalate) sample have the form of

pits with a mean diameter of 7 nm (Fig. 3). A somewhat different situation is observed on the surface of the mica (inorganic polymer) sample irradiated with xenon ions and decorated with gold (Fig. 4). In this case, new rounded structures (bumps) 40–50 nm in diameter can be seen on the surface.

The X-ray scattering curve measured for the surface of fused silica irradiated with xenon ions has two steps (Fig. 5). The first step corresponds to a distance of 63 nm, and the second step is associated with a distance of ~25 nm. It seems likely that the second distance corresponds to the diameter of the track core (channel). Similar results were obtained for leucosapphire.

Thus, it has been established that irradiation with high-energy particles brings about structural transformations in polymers. The degree and character of these transformations depend on the polymer nature. In particular, irradiation leads to the amorphization of poly(ethylene terephthalate) and polycarbonate and the crystallization of polyimide. In all the polymers studied, the macromolecules are oriented along the ion tracks. Graphite or a graphite-like material was found in the regions of latent-track cores. The surface morphology of polymers, mica, quartz, and leucosapphire was investigated. It was demonstrated that the size of tracks—regions of a modified material in polymers and crystals—depends on the energy of multiply charged heavy ions and can be as large as 50 nm.

SURFACE AND THE PHYSICAL PROPERTIES OF CRYSTALS IRRADIATED WITH ACCELERATED, MULTIPLY CHARGED, HEAVY IONS

The radiation damage in crystals can be described only through the displacement of individual atoms [13]. It is worth noting that, under high-energy irradiation, there arises a cascade of atomic displacements [14]. The return of atoms to an equilibrium state is encouraged by the transfer of additional energy to the crystal, for example, upon heating (annealing) or additional irradiation.

Among the crystals studied, leucosapphire is of special interest as a convenient model compound for studying radiation-induced phenomena associated with the atomic displacements and changes in the electron states [15]. It should be noted that, in the papers published thus far, no consideration has been given to the influence of the crystallographic factors (crystal orientation, irradiation direction) on the properties of irradiated surfaces. However, it is reasonable to assume that anisotropy of crystals should manifest itself upon their exposure to hard radiation.

We analyzed how the exposure of crystals to irradiation with high-energy Xe, Kr, Ar, and Bi heavy ions at energies of 1–3.5 MeV/amu (Flerov Laboratory of Nuclear Reactions, Joint Institute for Nuclear Research) affects the structure and properties of sapphire crystals with different crystallographic orientations. We studied samples of four types, namely, leucosapphire crystals whose surfaces were oriented along the (0001) (*z*), $(10\bar{1}0)$ (*m*), $(10\bar{1}2)$ (*r*), and $(11\bar{2}0)$ (*a*) crystallographic planes. No surface tracks were observed upon exposure of leucosapphire crystals to irradiation with krypton or xenon ions at energies up to 350 MeV or with bismuth ions at energies of less than 200 MeV. We only revealed a change in the integrated surface roughness. However, irradiation of the crystals with bismuth ions at energies of more than 200 MeV led to the formation of surface defects. The fine structure of these defects was thoroughly examined using atomic force microscopy (Fig. 6). It is important to note that the geometric parameters of the structures formed (such as the diameter, height, and depth of craters) depend substantially on the crystallographic orientation of the samples. Thus, it can be stated that we managed for the first time to elucidate how the crystallographic orientation of the samples affects their properties upon irradiation with high-energy heavy ions.

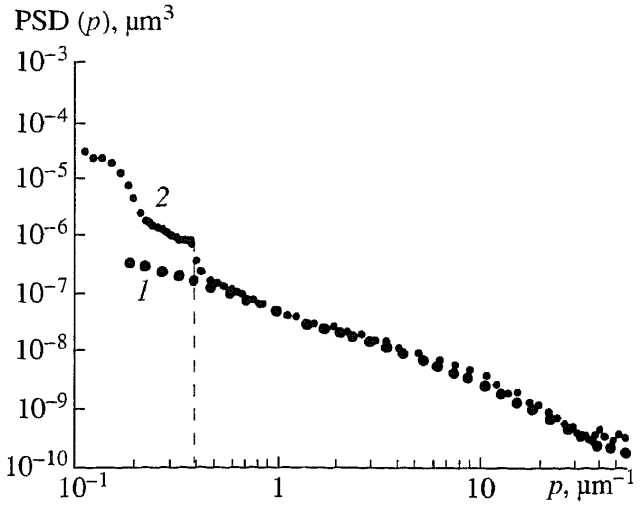

Fig. 5. X-ray scattering curves for the surface of fused silica (*1*) prior to and (*2*) after irradiation with high-energy ions.

For the most part, the results summarized in this section were obtained using thermally stimulated exoelectron emission—a nondestructive technique of measurement and testing that is sensitive to the surface condition of samples [16, 17].

The analysis of the results obtained in investigations into the radiation damage with the use of thermally stimulated exoelectron emission allowed us to draw the following inferences:

(i) The temperature dependence of the thermally stimulated exoelectron emission is governed by the crystallographic orientation of the sample. This can be explained by the fact that surfaces with different crystallographic orientations have traps (structural defects) characterized by different energy depths.

(ii) Irradiation of the surface of a leucosapphire crystal with high-energy heavy ions brings about a

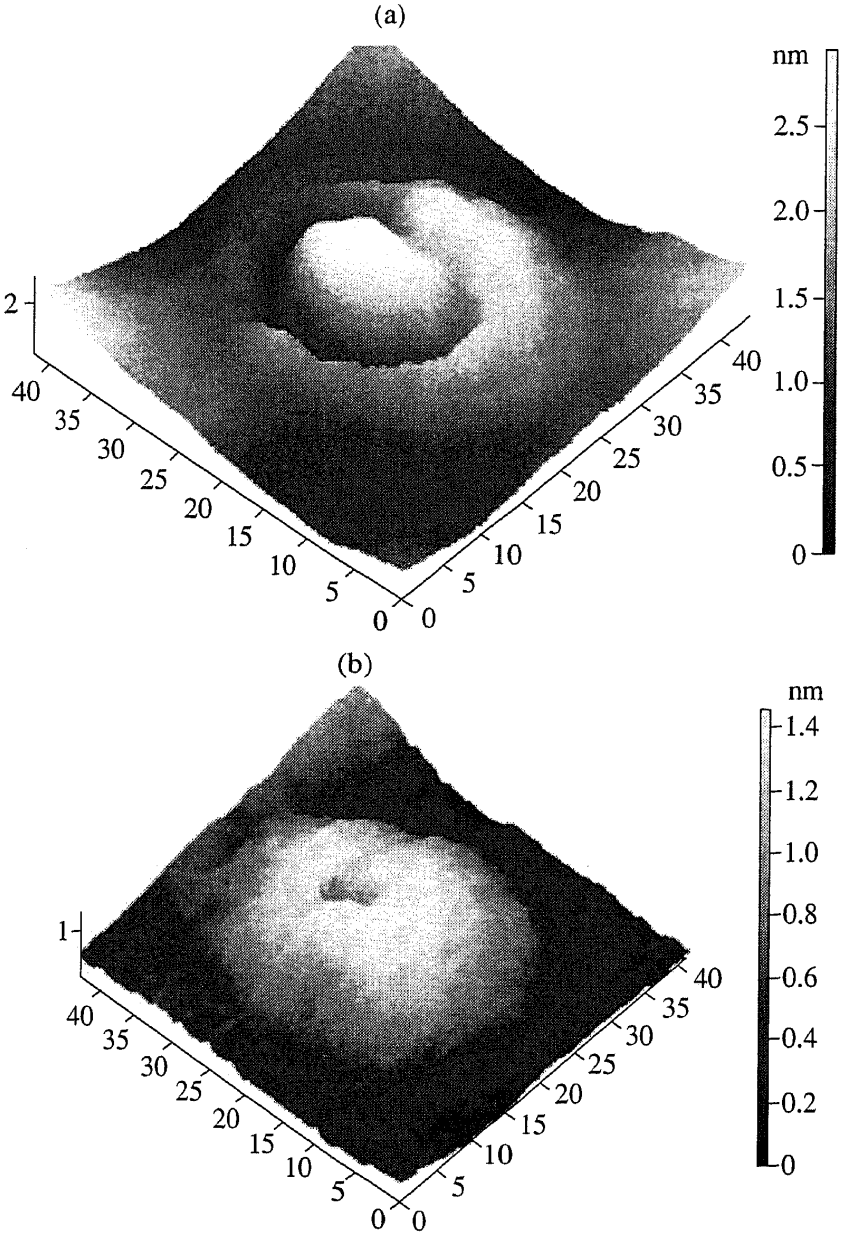

Fig. 6. AFM images of the surface of the leucosapphire crystal irradiated with bismuth ions at energies of (a) 300 and (b) 710 MeV.

change in the exoemission characteristics of the surface. This is associated with the formation of new defects and the change in the energy state of the surface.

(iii) The parameters of thermally stimulated exoelectron emission depend on the irradiation dose. An increase in the ion fluence leads to the following changes: the low-temperature emission peak observed in the range 200–300°C disappears, whereas the intensity of the high-temperature peaks revealed in the range 400–500°C increases. This pattern is observed for all the studied orientations of the samples. Moreover, it should be noted that the sample whose image is reproduced in Fig. 6a is characterized by two closely spaced high-temperature peaks. The intensity ratio of these peaks also depends on the irradiation dose.

In our opinion, the revealed temperature dependence of the thermally stimulated exoelectron emission can be used as an effective tool for determining the orientation of crystal faces.

SECONDARY NANOSTRUCTURES PREPARED ON THE BASIS OF TRACK MEMBRANES—NEW TYPES OF RAMAN-ACTIVE SURFACES

One of the most extensively used techniques of template synthesis of secondary nanostructures (such as cylindrical or tapered tips, hollow nanotubes, and nanowires) is electrochemical filling of pores of track membranes [4]. According to this technique, a 10- to 50-nm-thick metal layer is thermally deposited onto the surface of a track nanomembrane and then is hardened electrolytically (galvanically). The metal layer on the

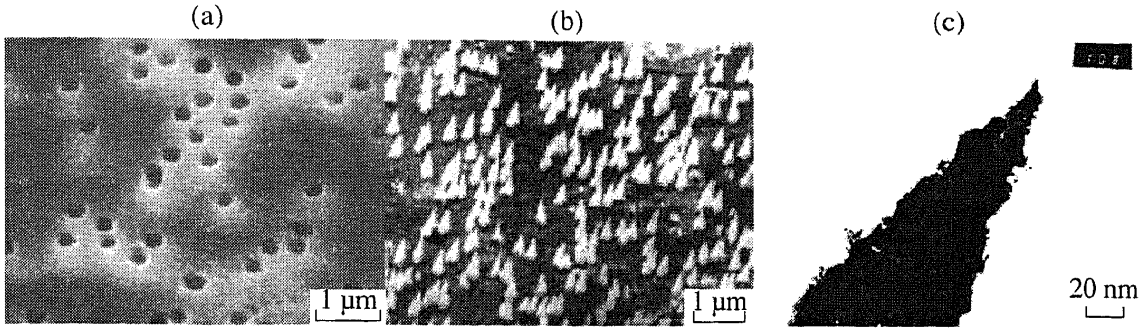

Fig. 7. Micrographs of (a) the metallized surface of the track membrane and (b) the structured metal (silver) surface with tapered tips (JEOL JSM-840 scanning electron microscope). (c) Micrograph of the apex of the tapered tip (JEOL JEM-100CX transmission electron microscope).

surface of the track membrane serves as a cathode. The duration and conditions of electrochemical filling of pores determine the degree of pore filling and, hence, the shape of secondary nanostructures, in particular, the nanowire length or the taper of the tip apex (Fig. 7).

Track metallic secondary nanostructures are universal Raman-active surfaces. The enhancement of Raman scattering on these surfaces does not depend on the properties of the applied sample of the material but is associated solely with the properties of the metallic surface [18, 19]. The enhancement of the Raman signal of test molecules located in the vicinity of this surface proceeds through the electromagnetic mechanism. This circumstance is of great importance in designing highly sensitive systems intended for detecting and analyzing, for example, trace amounts of biomacromolecules with a high sensitivity.

The surface-enhanced Raman spectra of the most characteristic compounds are shown in Fig. 8. In all cases, the surface-enhanced Raman spectra are similar to the Raman spectra of the compounds under investigation. This confirms the dominant role of the electromagnetic mechanism of enhancement on Raman-active surfaces prepared using the technique of replicas from pores of track membranes. In virtually all the cases, it was possible to detect a reliable signal from the sample containing ~1 pg of the material.

The surface-enhanced Raman spectra of lysozyme protein, which were recorded using the tip surface (spectrum *6*) and a silver electrode roughened in the course of the redox cycle accomplished in an electrochemical cell at a zero-charge potential of silver (spectrum *5*) [19], are compared in Fig. 8. The most intense bands in the surface-enhanced Raman spectra of the lysozyme adsorbed on the silver electrode correspond to vibrations of its constituent aromatic amino-acid residuals. It is worth noting that this spectrum does not exhibit bands characteristic of vibrations of phenylalanine in the vicinity of 1000 cm^{-1}. A lysozyme molecule has the shape of an ellipsoid $45 \times 30 \times 30$ $Å^3$ in size and involves three phenylalanine residuals (Phe^3, Phe^{34}, Phe^{38}). However, signals from these residuals located inside the protein globule do not manifest themselves, because the enhancement of Raman scattering in the Raman-active system of the silver electrode predominantly occurs through the molecular (i.e., short-range compared to the size of the protein molecule) mechanism [20].

Therefore, the use of the Raman-active surfaces prepared by making replicas from track membranes provides a means for recording the surface-enhanced Raman spectra of different chemical compounds in picogram amounts. Thus, we demonstrated that the Raman-active system proposed is universal, is characterized by the electromagnetic mechanism of Raman scattering enhancement, and can be used to increase the sensitivity of the recording of Raman spectra.

APPLICATION OF TRACK NANOMEMBRANES (CLEANING OF CRYSTALLIZATION SOLUTIONS)

Zaitseva *et al.* [21–23] noted that, in order to prepare successfully large-sized (with linear sizes of 50 cm or more) perfect potassium dihydrogen phosphate (KDP) crystals through the rapid-growth technique, it is necessary to perform not only preliminary membrane filtration of a crystallization solution but also a continuous membrane filtration of this solution in the course of growth. Wang *et al.* [24] analyzed the reasons for the necessity of conducting this operation. It was found that, upon addition of a cation impurity (sodium), the concentration of scattering centers in the KDP crystals grown increases in proportion to the impurity concentration and the characteristic sizes of the particles detected fall in the range 10–100 nm. As a consequence, these particles, for the most part, could not be retained by membranes (used for the preliminary filtration of the crystallization solution) with a pore diameter of 0.22 μm. However, closer examination revealed that impurity particles of these sizes are hard to incorporate into the growing crystal but enter together with inclusions of the crystallization solution. This can lead to the formation of scattering regions whose sizes substantially exceed the diameter of pores in the membranes used. Apparently, this circumstance is the reason is why

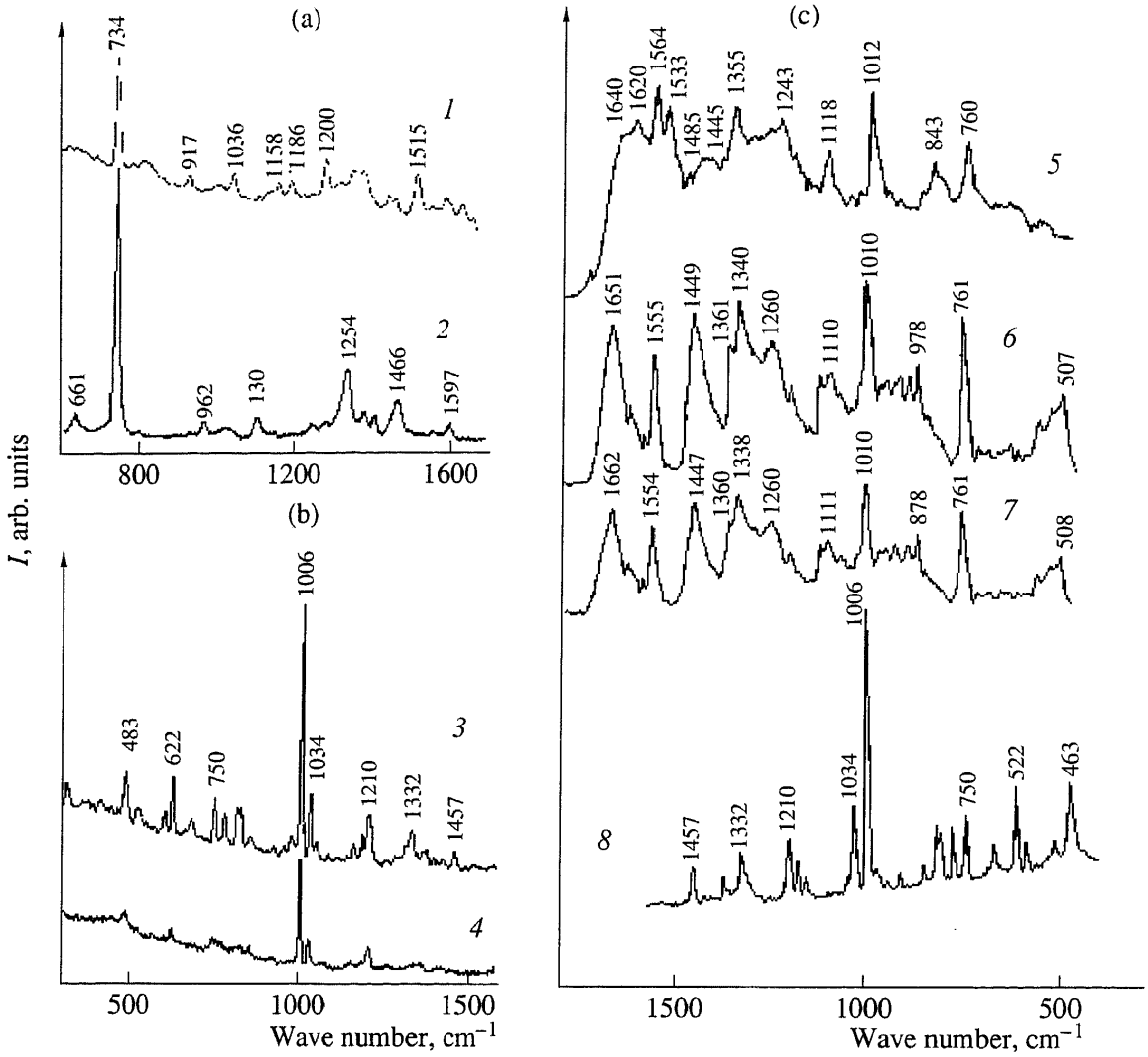

Fig. 8. Surface-enhanced Raman spectra recorded using Raman-active surfaces prepared by the track membrane technique (silver; tip diameter $d = 30$ nm; height-to-diameter ratio of tips $h/d = 2$; surface density of tips, 10^{11} cm^{-2}). (a) Surface-enhanced Raman spectra of (*1*) thymus deoxyribonucleic acid and (*2*) adenosine monophosphate on the tip surface. The amount of the compound in the sample is 1 pg. (b) Comparison of (*3*) the surface-enhanced Raman spectrum of the phenylalanine sample (the amount of the compound used for recording the spectrum is 1 pg) with (*4*) the Raman spectrum of the phenylalanine sample (the amount of the compound used for recording the spectrum is 1 mg). (c) Surface-enhanced Raman spectra of the lysozyme protein on (*5*) the silver electrode and (*6*) the tip surface, (*7*) Raman spectrum of lysozyme, and (*8*) surface-enhanced Raman spectrum of phenylalanine (shown on the same scale for comparison). The amounts of lysozyme and phenylalanine in the samples on the tip surface and the amount of lysozyme in the sample on the electrode are equal to 1 pg. The lysozyme concentration in an aqueous solution is 25 mg/ml. The excitation wavelength is 514.5 nm. The excitation powers used for recording the surface-enhanced Raman and Raman spectra are equal to 20 and 250 mW, respectively.

membrane with pore diameters of 0.5 and 0.02 μm were successively used for the filtration during the growth of large-sized, highly perfect KDP crystals with an increased resistance to laser radiation at a wavelength of 0.355 μm [23].[1] The main feature distinguishing track membranes from traditional membranes is that their pores have a regular and controlled structure and geometry. From the outset, this rendered track membranes attractive for use in cleaning of aqueous crystallization solutions [25, 26].

Let us now consider our data on the filtration of solutions used for the growth of KDP crystals [27, 28]. We examined poly(ethylene terephthalate) track membranes with pore sizes of 0.1–4 μm. Preliminary cleaning was carried out using poly(ethylene terephthalate) track membranes with pore sizes of 1–4 μm, and the final cleaning of water and the solutions of KDP crystals prepared from raw materials of different batches in which the content of controllable impurities was less than 10^{-4}–10^{-5} wt % was performed with poly(ethylene

[1] The minimum size of pores in these membranes was most likely chosen reasoning from the necessity of growing crystals suitable for use as highly transparent optical elements in the visible and near-IR spectral ranges. For this purpose, it was desirable to provide appropriate conditions for Rayleigh scattering by impurity particles (the particle size must be considerably less than the radiation wavelength) in solutions and, correspondingly, in crystals.

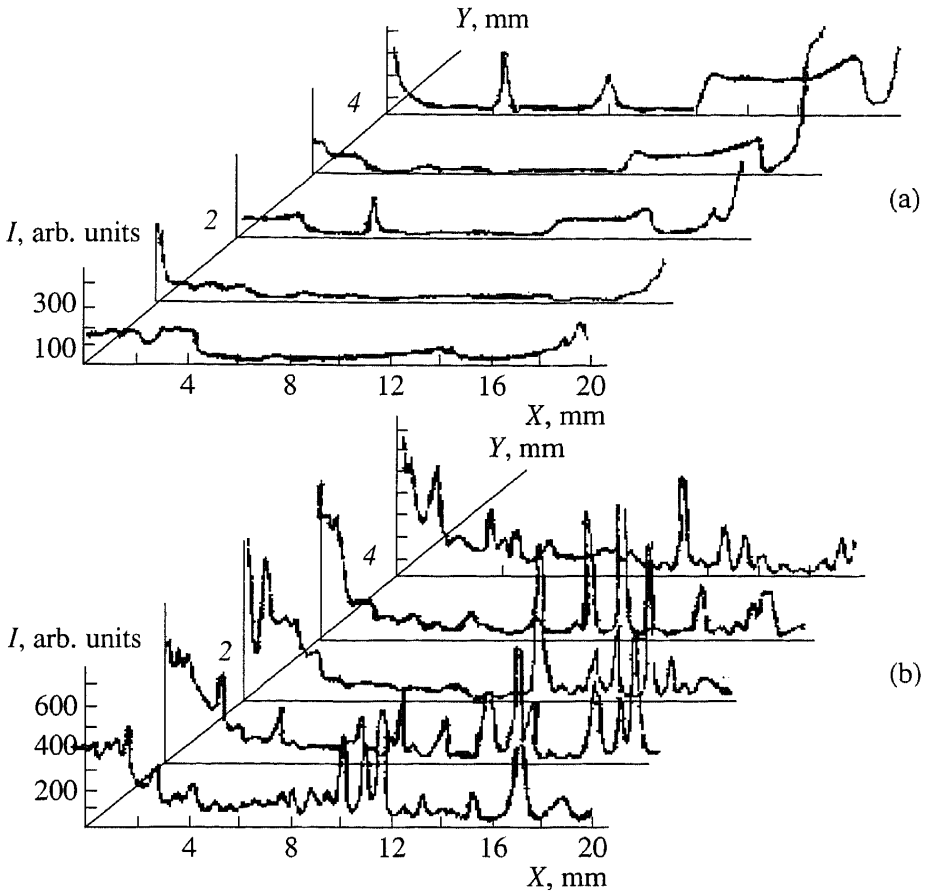

Fig. 9. Light scattering curves ($\lambda = 0.63$ μm) for the middle cross section of the potassium dihydrogen phosphate crystals grown (a) from a solution filtered through track membranes with a pore size of 0.5 μm and (b) from a nonfiltered solution.

terephthalate) track membranes whose pore sizes were equal to 0.1–0.5 μm. The analysis of the elemental composition revealed the presence of glass fragments, fibers, organic films, and biological substances. The intensity of UV scattering both from water used for preparing crystallization solutions and from the crystallization solutions themselves was investigated as a function of the diameter of the pores involved in the track membranes. These investigations demonstrated that the use of membranes with pore diameters from 1 to 0.05 μm decreases the intensity of scattering from the crystallization solution significantly (by several orders of magnitude).

Our investigations of the KDP crystals grown using traditional membranes characterized by a large spread in pore diameters revealed that these crystals contain inclusions of microobjects with sizes up to 10–15 μm. At the same time, the characteristic sizes of similar objects in the KDP crystals grown with the use of track membranes completely correspond to the diameters of pores involved in these membranes.

According to experimental data on the intensity of visible-light scattering by KDP crystals grown from a nonfiltered solution and a solution subjected to successive filtration through track membranes with pore diameters of 1 and 0.5 μm, the crystals grown from the filtered solution have a substantially higher optical quality and homogeneity (Fig. 9). The use of track membranes made it possible to decrease the scattering intensity in the visible spectral range by more than one order of magnitude, whereas the degree of inhomogeneity of the crystals grown was reduced by a factor of five. These results were obtained for the KDP crystals grown at very high rates (up to 50 mm/day). Thus, the problem of rapid growth of perfect water-soluble crystals is closely associated with the development of membrane filtration methods.

CONCLUSIONS

The above results have demonstrated that investigations into the interaction of high-energy beams (primarily formed by fission fragments, heavy ions, synchrotron radiation, fullerenes, and aggregates of colloidal particles) with materials forming matrices of nanopore systems (polymers, crystals) are of considerable importance from scientific and practical standpoints. The results obtained in these investigations will make it possible to control the parameters of pores in track membranes and to modify the properties of irradiated crystals and secondary nanostructures synthesized using track membranes. This will provide the basis for the design of more efficient track nanomembranes with

improved technological characteristics. To date, it has been established that track nanomembranes (with pore sizes of 3–30 nm) can be used to selectively separate complex multicomponent ion solutions and isolate (clean and concentrate) proteins (with molecular masses of 20–200 kDa) and small-sized (approximately 20–30 nm) viruses. Track nanomembranes can serve as active elements in multipurpose biosensors (in particular, those designed for determining a total water pollution, revealing the presence of viruses and bacteria in water, and performing a quantitative analysis for sugar in a blood). Track nanomembranes are the main components of life-support systems in modern clean rooms.

ACKNOWLEDGMENTS

We would like to thank Kh.S. Bagdasarov, A.É. Voloshin, and A.L. Tolstikhina (Shubnikov Institute of Crystallography, Russian Academy of Sciences); Yu.Ts. Oganesyan, S.N. Dmitriev, P.Yu. Apel', V.A. Skuratov, and V.F. Reutov (Flerov Laboratory of Nuclear Reactions, Joint Institute for Nuclear Research); V.O. Naĭdenov, L.G. Karpukhina, M.F. Kudoyarov, and G.M. Gusinskiĭ (Ioffe Physicotechnical Institute, Russian Academy of Sciences); V.A. Romanov, B.I. Fursov, and G.S. Zhdanov (Institute of Physics and Power Engineering, State Research Center); V.M. Golovkov (Research Institute of Nuclear Physics, Tomsk State Polytechnical University); V.F. Pendyurin and V.P. Naz'mov (Institute of Nuclear Physics, Siberian Division, Russian Academy of Sciences); V.D. Shestakov and V.I. Kuznetsov (Research Center for Applied Nuclear Physics, Ministry of Nuclear Energy of the Russian Federation); A.N. Cherkasov and A.E. Polotskiĭ (State Research Institute of Highly Pure Biopreparations, Scientific Center, Ministry of Public Health of the Russian Federation); and Yu.M. Evdokimov (Éngelhardt Institute of Molecular Biology, Russian Academy of Sciences) for supplying track membranes, crystals, and biopolymers used in our experiments and also for their help in analyzing the properties of materials and their cooperation in the development of practical application of track membranes and secondary nanostructures.

The series of investigations performed in 1983–2003 was supported by the Ministry of Science and Technology of the Russian Federation, the Russian Foundation for Basic Research, International Center of Science and Technology, and the International Association of Assistance for the promotion of cooperation with scientists from the New Independent States of the former Soviet Union (INTAS).

REFERENCES

1. *Nanotechnology Research Directions: Nanotechnology in the Next Decade*, Ed. by M. C. Roco, R. S. Williams, and R. Alivisatos (Kluwer Academic, Dordrecht, 2000; Mir, Moscow, 2002).
2. P. B. Price and R. M. Walker, Phys. Rev. Lett. **8**, 217 (1962).
3. G. N. Flerov and V. S. Barashenkov, Usp. Fiz. Nauk **114** (2), 351 (1974) [Sov. Phys. Usp. **17**, 783 (1975)].
4. B. V. Mchedlishvili, V. V. Beryozkin, V. A. Oleinikov, *et al.*, J. Membr. Sci. **79**, 285 (1993).
5. Ch. R. Martin, Science **206**, 1961 (1994).
6. L. Dauginet-De Pra, R. Ferain, R. Legras, and S. Demoustier-Champagne, Nucl. Instrum. Methods Phys. Res. B **196**, 81 (2002).
7. G. N. Flerov, Vestn. Akad. Nauk SSSR, No. 4, 35 (1984).
8. P. Yu. Apel, Nucl. Tracks Radiat. Meas. **6**, 115 (1982).
9. G. I. Distler, V. P. Vlasov, Yu. M. Gerasimov, *et al.*, *Decoration of Solid Surfaces* (Nauka, Moscow, 1976).
10. V. E. Asadchikov, Yu. A. Karabekov, V. V. Klechkovskaya, *et al.*, Kristallografiya **43** (1), 119 (1998) [Crystallogr. Rep. **43**, 110 (1998)].
11. V. A. Alekseev, N. N. Mel'nik, and S. A. Voronov, in *Proceedings of the International Conference "Raman Scattering Effect 98"* (Moscow, 1998), p. 111.
12. I. P. Kozlov, V. B. Odzhaev, N. B. Popok, *et al.*, J. Appl. Spectrosc. **65**, 583 (1998).
13. S. A. Durrani and R. K. Bull, *Solid State Nuclear Track Detection: Principles, Methods, and Applications* (Pergamon, Oxford, 1987; Énergoatomizdat, Moscow, 1990).
14. Ch. Lehmann, *Interaction of Radiation with Solids and Elementary Defect Production* (North-Holland, Amsterdam, 1977; Atomizdat, Moscow, 1979).
15. G. P. Pells, J. Am. Ceram. Soc. **77** (2), 368 (1994).
16. V. S. Kortov, A. I. Slesarev, and V. V. Rogov, *Emission Control of the Surfaces of Parts after Their Treatment* (Naukova Dumka, Kiev, 1986).
17. V. V. Shorin, in *Proceedings of the Symposium on Exoemission* (Lvov, 1989), p. 27.
18. M. Fleishmann, P. J. Hendra, and A. J. McQuillan, J. Chem. Soc., Chem. Commun. **8**, 80 (1973).
19. K. Kneipp, H. Kneipp, P. Corio, *et al.*, Phys. Rev. Lett. **84** (15), 3470 (2000).
20. I. R. Nabiev, G. D. Chumanov, and R. G. Efremov, J. Raman Spectrosc. **21** (1), 49 (1990).
21. N. P. Zaitseva, L. N. Rashkovich, and S. V. Bogatyreva, J. Cryst. Growth **148**, 276 (1995).
22. N. P. Zaitseva, J. J. De Yoreo, M. R. Dehaven, *et al.*, J. Cryst. Growth **180**, 255 (1997).
23. N. Zaitseva, J. Atherton, R. Rozsa, *et al.*, J. Cryst. Growth **197**, 911 (1999).
24. S. Wang, Z. Gao, Y. Fu, *et al.*, J. Cryst. Growth **223**, 415 (2001).
25. V. I. Bredikhin, A. B. Vasil'ev, G. L. Galushkina, *et al.*, Vysokochist. Veshchestva, No. 2, 116 (1990).
26. N. P. Zaĭtseva, I. L. Smol'skiĭ, and L. N. Rashkovich, Kristallografiya **36** (1), 198 (1991) [Sov. Phys. Crystallogr. **36**, 113 (1991)].
27. B. V. Mchedlishvili, V. V. Berezkin, A. B. Vasil'ev, *et al.*, in *Physical Crystallography* (Nauka, Moscow, 1992), p. 43.
28. A. B. Vasil'ev, A. É. Voloshin, and V. V. Dolbinina, in *Proceedings of the All-Russia Scientific Conference "Membranes-2001"* (Moscow, 2001), p. 86.

Translated by O. Borovik-Romanova